Department of Orthopedics[1], China-Japan Union Hospital of Jilin University; Department of Ophthalmology[2], The Second Hospital of Jilin University, Changchun, China

MicroRNA-489-3p inhibits neurite growth by regulating PI3K/AKT pathway in spinal cord injury

Rui Jiang[1], Chao Zhang[2], Rui Gu[1], Han Wu[1,*]

Received December 14, 2016, accepted January 19, 2017

**Corresponding author: Han Wu, Department of Orthopedics, China-Japan Union Hospital of Jilin University, No.126, Xiantai Street, Changchun 130033, China*
wuhan873@126.com

Pharmazie 72:272–278 (2017) *doi: 10.1691/ph.2017.6972*

Spinal cord injury (SCI) is caused by mechanical disruption of the spinal cord. This primary injury is followed by a devastating secondary SCI. It has been shown that various microRNAs (miRNAs) are involved in secondary SCI. The present study explored the role of miR-489-3p on secondary SCI, and its underlying mechanisms. First, we determined the expression of miR-489-3p in blood samples of SCI patients and healthy controls. Further experiments were performed on human neural cell lines, treated with bupivacaine to induce neuron damage. The cultured neural cells were transfected with miR-489-3p mimic, ASO-miR-489-3p or negative control. We then measured cell proliferation and apoptosis in cultured neurons, followed by measurement of neurite outgrowth. After confirming NAA10 as a target gene for miR-489-3p, we measured expression of NAA10 in neurons transfected with miR-489-3p. Finally, we evaluated the effects of miR-489-3p on the PI3K/AKT signal pathway. miR-489-3p was highly expressed in SCI patients and in bupivacaine-treated injured neurons. In cell model, miR-489-3p inhibited proliferation of neurons and promoted apoptosis. miR-489-3p and bupivacaine synergistically inhibited neurite growth. NAA10 gene was negatively regulated by miR-489-3p. Overexpression of NAA10 reversed the effects of miR-489-3p on neurons. Lastly, we found that the inhibitory effects of miR-489-3p on neurons are mediated via activation of the PI3K/AKT pathway. Inhibition of PI3K/AKT pathway using miR-489-3p inhibitor reversed the effects of miR-489-3p on neurons.

1. Introduction

Spinal cord injury (SCI) is a devastating and debilitating injury which is primarily caused by a mechanical disruption of the spinal cord, resulting into quick death of neurons and glia. The primary traumatic injury to spinal cord is followed by a multifactorial secondary injury which is long in duration and more devastating. This secondary injury is induced by multiple processes, including neuronal and glial apoptosis, inflammation, glial scar formation, local edema/ischemia, and oxidative stress (Bareyre 2008; Donnelly and Popovich 2008). Due to the irreversibility of primary SCI, treatment strategy should target the secondary SCI, which plays a critical role in the recovery of function (Calvo et al. 2011). Therefore, development of innovative therapeutic strategies to reduce secondary SCI depends on a proper understanding of secondary injury mechanisms at molecular and biochemical levels.

MicroRNAs (miRNAs) are small, non-coding RNAs composed of approximately 20 to 24 nucleotides that regulate the expression of protein-encoding genes at post-transcriptional level. miRNAs are involved in various cellular processes such as cell proliferation, apoptosis, and differentiation (Bartel 2004; Bhalala et al. 2013; Slezak-Prochazka et al. 2010). It has been reported that miRNAs play key roles in the process of nerve development and injury repair (Bhalala et al. 2013; Hutchison et al. 2009; Wu and Murashov 2013). In a microarray study in rats, more than 35% of the miRNAs expressed in the spinal cord were significantly affected within the first seven days following injury, with some miRNAs showing a sustained increase in expression and others showing a sustained decrease (Nai-Kui Liu 2009).

Roles of several miRNAs in SCI have been evaluated in animal studies. In a murine transection model of SCI, infusion of miR-20a into the normal spinal cord induced inflammation and neuronal cell death, similar to that observed after SCI. Inhibition of miR-20a decreased the effects of SCI, by improving hindlimb motor recovery and decreasing neuronal death (Jee et al. 2012). Similar effects were observed for miR-486 in a murine contusion model of SCI. Infusion of miR-486 into the uninjured spinal cord induced SCI-like effects, with increased neuronal death and decreased motor function (Min et al. 2012). In another murine contusion model of SCI, miR-21 levels increased slightly around the lesion site within the first two weeks after injury. However, as the injury response progressed, miR-21 levels were greatly upregulated (Bhalala et al. 2012).

It has been reported that miR-489-3p (also known as miR-489) plays an important role in several cancers (Liu et al. 2016; Patel et al. 2016; Xie et al. 2015; Zhang et al. 2016). miR-489-3p is also reported to regulate cardiac hypertrophy (Wang et al. 2014). To our best knowledge, role of miR-489-3p in nervous system or SCI is not yet studied. Thus, we explored the functional role of miR-489-3p in SCI, as well as underlying mechanisms.

2. Investigations and results

2.1. miR-489-3p is highly expressed in SCI

Serum from 20 patients with SCI and 20 healthy controls were collected. qRT-PCR was used to measure expression level of miR-489-3p among patients and healthy controls. As shown in Fig. 1A, levels of miR-489-3p expression in patients with SCI was significantly higher than that in control ($p<0.05$).

Bupivacaine at different concentrations (0, 0.5, 1, 2, 5, and 10 mM) was used to induce neuronal injury in human neural cells, AGE1. HN and SY-SH-5Y. Expression level of miR-489-3p was then measured in these injured neurons using qRT-PCR. As shown in Fig. 1B, expression of miR-489-3p in the injured cultured neurons was significantly increased with increasing doses of bupivacaine, with highest level at 10 mM concentration.

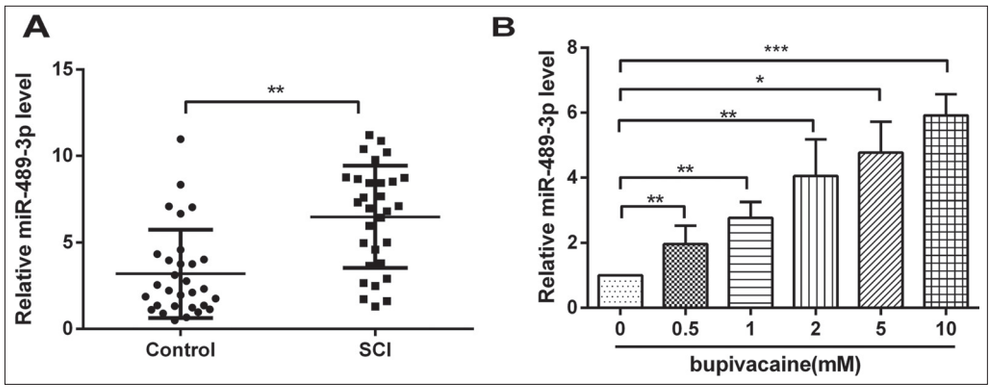

Fig. 1: miR-489-3p is highly expressed in SCI. Quantitative RT-PCR was performed to examine differential expression of miR-489-3p in SCI patients versus healthy controls (A) and bupivacaine-treated human neural cells (B). RT-PCR: Reverse transcription polymerase chain reaction; SCI: spinal cord injury. * P<0.05, ** P<0.01, *** P<0.001.

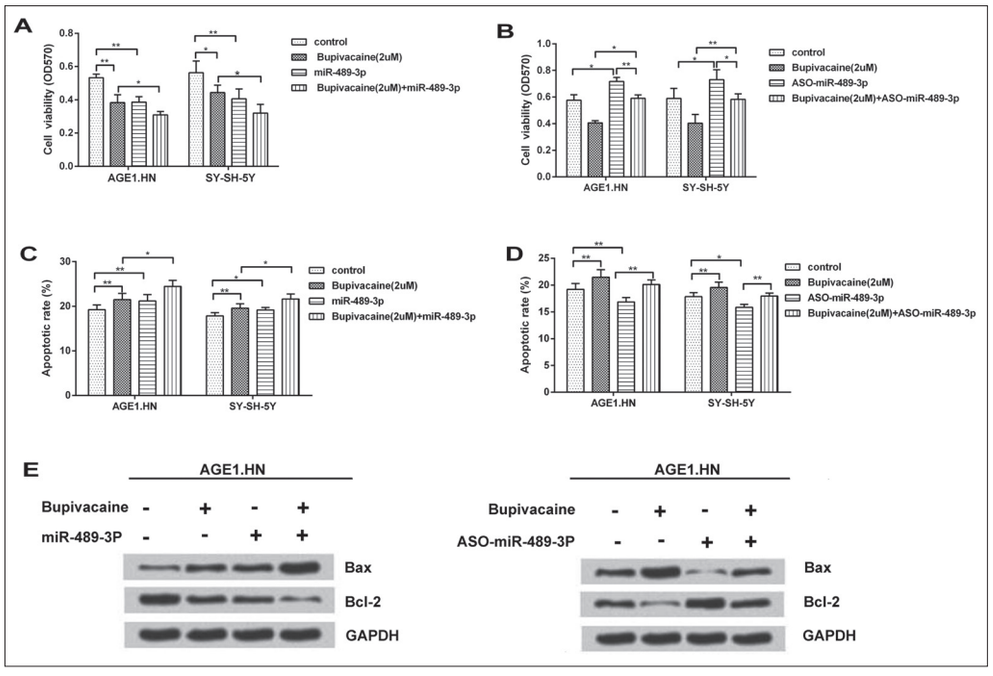

Fig. 2: miR-489-3p inhibits proliferation and promotes apoptosis of neural cells. Viability and apoptosis of neural cells were measured using MTT assay (A and B) and flow cytometry (C and D), respectively. In panels A and C, the cells were transfected with control, bupivacaine, miR-489-3p mimic, or bupivacaine plus miR-489-3p. In panels C and D, the cells were transfected with control, bupivacaine, ASO-miR-489-3p mimic, or bupivacaine plus ASO-miR-489-3p. (E) Western blot analysis was used to measure expressions of Bax and Bcl-2 in AGE1.HN cells. GAPDH: glyceraldehyde-3-phosphate dehydrogenase; MTT: 3-(4,5-dimethylthiazol-2-yl)-2 5-diphenyl-2Htetrazolium bromide. * P<0.05, ** P<0.01, *** P<0.001.

Thus, Fig. 1A and 1B together confirm that expression level of miR-489-3p is increased in neurons after SCI.

2.2. miR-489-3p inhibits proliferation and promotes apoptosis of neural cells

To test whether miR-489-3p can affect neural cells, we determined the impact of miR-489-3p on cell proliferation and apoptosis. Cell proliferation was measured using MTT assay and apoptosis was measured using flow cytometry.

As shown in Fig. 2A, both bupivacaine (2 mM) and miR-489-3p mimic significantly decreased cell viability as compared to control (both p<0.05); the mixture of bupivacaine and miR-489-3p mimic further decreased viability (p<0.05). However, knockdown of miR-489-3p expression using ASO-miR-489-3p reversed this effect and increased cell viability significantly (p<0.05; Fig. 2B).

Both bupivacaine and miR-489-3p mimic significantly increased apoptosis as compared to control (both p<0.05; Fig. 2C); the mixture of bupivacaine and miR-489-3p mimic further increased apoptosis (p<0.05; Fig. 2C). However, knockdown of miR-489-3p expression reversed this effect and decreased apoptosis significantly (p<0.05; Fig. 2D). Additionally, we also explored the mechanism underlying this apoptotic effects. Western blot analysis was used to determine expression levels of pro-apoptotic protein (Bax) and anti-apoptotic protein (Bcl-2) in AGE1.HN cells. As shown in Figs. 2E, overexpression of miR-489-3p combined with bupivacaine increased Bax expression but decreased Bcl-2 expression, while knockdown of miR-489-3p reversed these effects. This finding shows that overexpression of miR-489-3p promotes apoptosis of nerve cells via modulation of expressions of apoptosis-related proteins, Bax and Bcl-2.

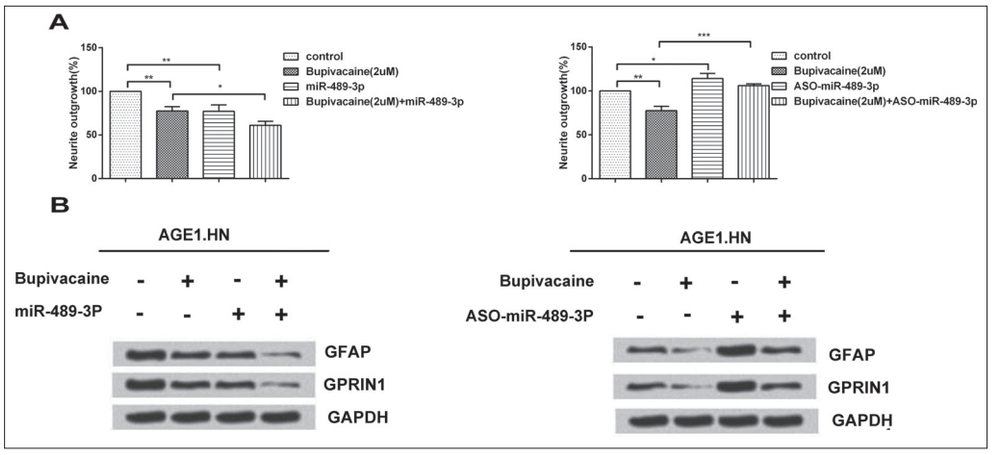

Fig. 3: miR-489-3p inhibits neurite outgrowth. The cells were transfected with control, bupivacaine, miR-489-3p mimic, bupivacaine plus miR-489-3p, ASO-miR-489-3p mimic, or bupivacaine plus ASO-miR-489-3p. (A) Neurite outgrowth assay was used to measure the rate of neurite outgrowth in cells. (B) Western blot analysis was used to measure expressions of GFAP and GPRIN1 in AGE1.HN cells. GFAP: glial fibrillary acidic protein; GPRIN1: G protein regulated inducer of neurite outgrowth 1; GAPDH: glyceraldehyde-3-phosphate dehydrogenase. * P<0.05, ** P<0.01, *** P<0.001.

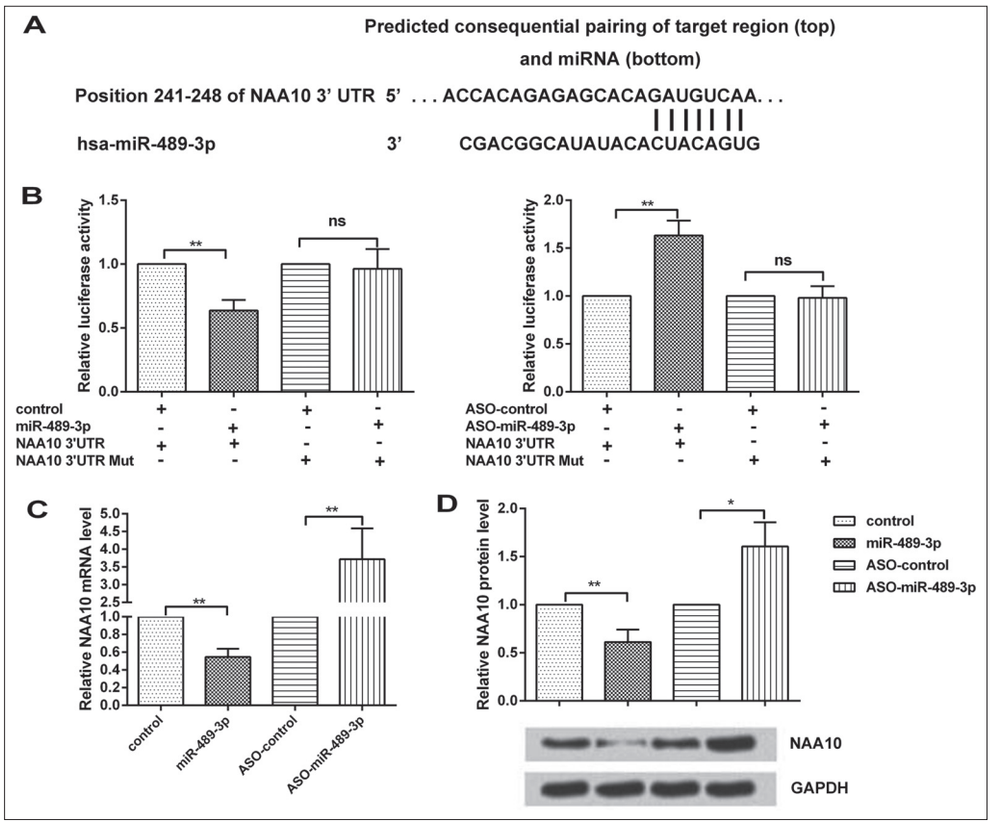

Fig. 4: NAA10 is down-regulated by miR-489-3p in neural cells. (A) Seed sequences of miR-489-3p in 3'UTR of NAA10 are indicated. (B) Neural cells were co-transfected with 3' UTR of NAA10 and miR-489-3p, 3' UTR of NAA10 and ASO-miR-489-3p, control, or mock and then relative luciferase activity was measured. (C) qRT-PCR was used to measure relative NAA10 mRNA level in cells transfected with control, miR-489-3p, ASO-control, or ASO-miR-489-3p. (D) Western blot analysis was used to measure relative NAA10 protein level in cells transfected with control, miR-489-3p, ASO-control, or ASO-miR-489-3p. qRT-PCR: quantitative reverse transcription polymerase chain reaction; GAPDH: glyceraldehyde-3-phosphate dehydrogenase; NAA10: N(alpha)-acetyltransferase 10. * P<0.05, ** P<0.01.

2.3. miR-489-3p inhibits neurite outgrowth

We then investigated whether the growth of neurite would also be inhibited by bupivacaine and miR-489-3p due to neurotoxicity. As shown in Fig. 3A, both bupivacaine and miR-489-3p mimic significantly decreased neurite outgrowth as compared to control (both p<0.05); the mixture of bupivacaine and miR-489-3p mimic further decreased neurite outgrowth (p<0.05). However, knockdown of miR-489-3p expression reversed this effect and increased neurite outgrowth significantly (p<0.05; Fig. 3A).

Furthermore, we also explored the mechanism underlying this inhibitory effect on neurite growth. Western blot analysis was used to determine expression levels of glial fibrillary acidic protein

(GFAP) and G protein regulated inducer of neurite outgrowth 1 (GPRIN1) in AGE1.HN cells. As shown in Figs. 3B, overexpression of miR-489-3p combined with bupivacaine decreased levels of GFAP and GPRIN1, while knockdown of miR-489-3p reversed this effect. This finding shows that overexpression of miR-489-3p inhibits neurite outgrowth via decreasing the expressions of GFAP and GPRIN1.

2.4. NAA10 is downregulated by miR-489-3p in neural cells

The putative seed sequences for miR-489-3p at the 3'UTR of NAA10 gene were indicated based on a bioinformatics analysis (Fig. 4A). Based on this finding, NAA10 was predicted as a target gene of miR-489-3p. To further confirm that NAA10 is a target gene of miR-489-3p, dual luciferase reporter assay was performed using AGE1.HN and SY-SH-5Y cells. As shown in Figure 4B, the luciferase activity was significantly decreased in cells co-transfected with miR-489-3p and 3'UTR of NAA10 as compared to the control sample ($p<0.05$). In contrast, the luciferase activity was significantly increased in cells co-transfected with ASO-miR-489-3p and 3'UTR of NAA10 as compared to the control ($p<0.05$; Fig. 4B). This finding suggests that miR-489-3p negatively regulates NAA10 gene expression.

Additionally, we performed qRT-PCR and Western blot analysis to reaffirm the effect of miR-489-3p on NAA10. The qRT-PCR results showed that miR-489-3p significantly decreased relative NAA10 mRNA level as compared to the control, while ASO-miR-489-3p increased NAA10 mRNA expression ($p<0.05$; Fig. 4C). Similar findings were observed in the Western blot analysis: miR-489-3p significantly decreased NAA10 protein expression as compared to the control, while ASO-miR-489-3p increased NAA10 protein expression ($p<0.05$; Fig. 4D).

2.5. NAA10 promotes neural cell proliferation, inhibits apoptosis and promotes neurite outgrowth

After confirming NAA10 as a target gene for miR-489-3p, we examined whether NAA10 could affect neurons proliferation and neurite outgrowth in presence of miR-489-3p. Figure 5A shows that NAA10 significantly improved viability of neurons as compared to the control ($p<0.05$), and also reversed the decreased cell viability induced by miR-489-3p ($p<0.05$). We then measured apoptosis using flow cytometry. As shown in Fig. 5B, NAA10 significantly inhibited apoptosis of neurons as compared to the control ($p<0.05$), and also reversed the miR-489-3p-induced apoptotic effect ($p<0.05$).

We then performed neurite outgrowth assay to evaluate effect of NAA10 on neurite outgrowth. As evident from Fig. 5C, NAA10 significantly promoted neurite outgrowth as compared to the control ($p<0.05$), and also reversed the inhibitory effect of miR-489-3p on neurite outgrowth ($p<0.05$). Earlier, we demonstrated that miR-489-3p inhibits neurite outgrowth via downregulating the expressions of GFAP and GPRIN1. Considering this finding, we measured the effect of NAA10 on these proteins using Western blot analysis. The results showed that NAA10 promoted the expression of these synaptic growth marker proteins, and could also reverse the inhibiting effect of miR-489-3p on these proteins (Fig. 5D).

2.6. miR-489-3p activates PI3K/AKT pathway

Lastly, we examined whether the phosphoinositide 3-kinase/serine-threonine kinase (PI3K/AKT) pathway could be involved in the inhibitory effects of miR-489-3p on neurons. Western blot analysis was used to determine the expression levels of PI3K, p-AKT, AKT, phosphorylated extracellular signal-regulated kinase-1 (p-ERK2), and ERK2 in neurons. As shown in Fig. 6A, miR-489-3p and bupivacaine increased the expressions of PI3K, p-AKT, and p-ERK2. However, knockdown of miR-489-3p partly inhibited the activation effects induced by bupivacaine (Fig. 6B). Figures 6C and 6D show the quantitative analysis of p-AKT and p-ERK, respectively. As shown in Fig. 6C, both miR-489-3p and bupivacaine alone or together significantly increased the expression of p-AKT as compared to the control ($p<0.05$); however, ASO-miR-489-3p significantly decreased the expression of p-AKT and also reversed the effect of bupivacaine ($p<0.05$). Similar results were observed for p-ERK, as evident from Fig. 6D. Thus, these findings together indicate that miR-489-3p exhibits its inhibitory effect on neurons by activation of the PI3K/AKT pathway.

3. Discussion

In our study, we found that miR-489-3p levels were significantly higher in SCI patients and in bupivacaine-treated injured neurons, indicating high expression of miR-489-3p after SCI. In the cell model, we found that miR-489-3p could inhibit proliferation of

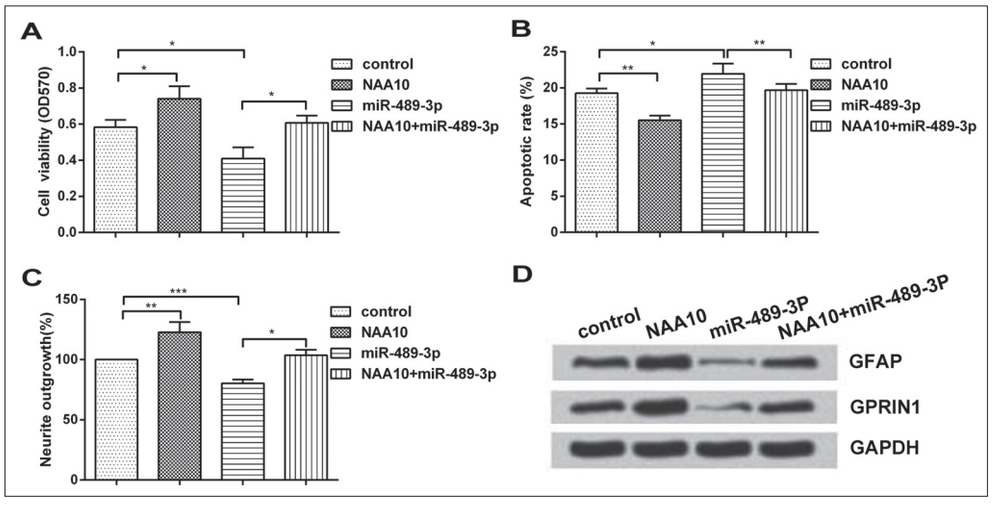

Fig. 5: NAA10 promotes neural cell proliferation, inhibits apoptosis and promotes neurite outgrowth. The neural cells were transfected with control, NAA10, miR-489-3p mimic, or NAA10 plus miR-489-3p. (A) MTT assay was used to measure viability of neural cells. (B) Flow cytometry was used to measure apoptosis in cells. (C) Neurite outgrowth assay was used to measure the rate of neurite outgrowth in neural cells. (D) Western blot analysis was used to measure expressions of GFAP and GPRIN1 in neural cells. GFAP: glial fibrillary acidic protein; GPRIN1: G protein regulated inducer of neurite outgrowth 1; GAPDH: glyceraldehyde-3-phosphate dehydrogenase; MTT: 3-(4,5-dimethylthiazol-2-yl)-2 5-diphenyl-2Htetrazolium bromide. * P<0.05, ** P<0.01, *** P<0.001.

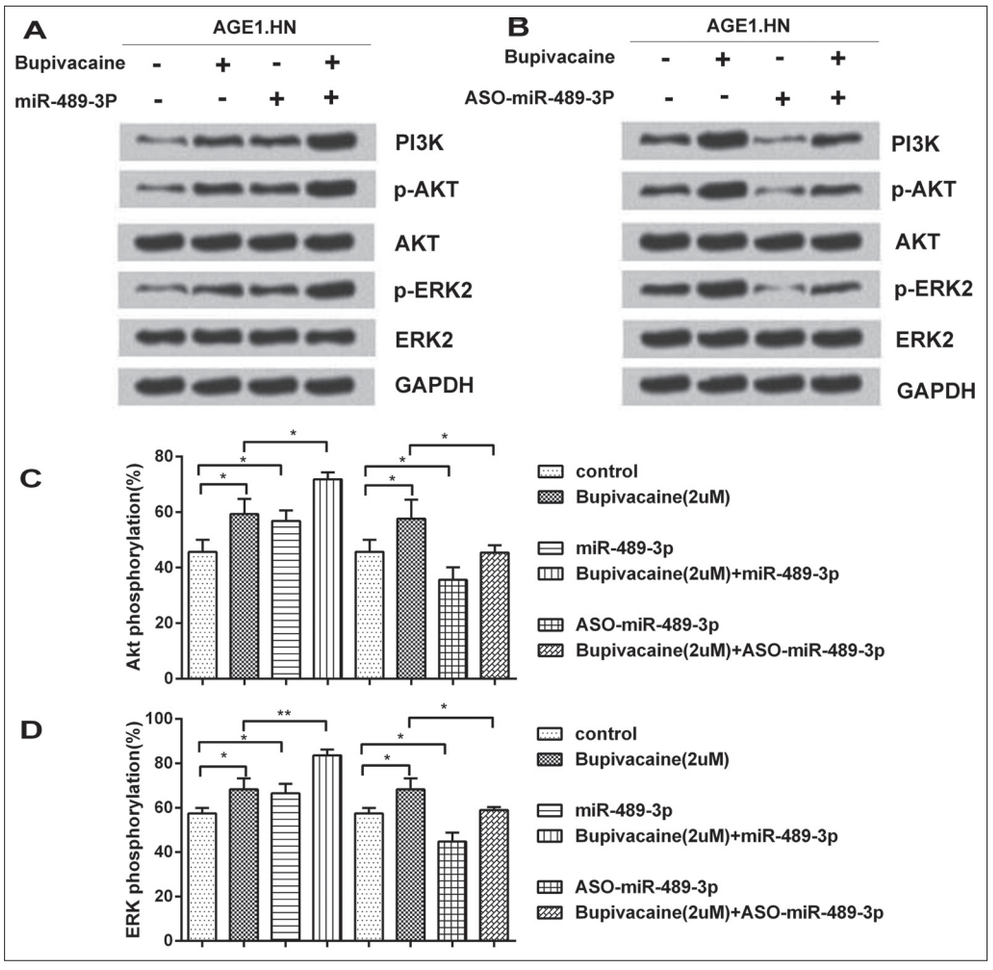

Fig. 6: miR-489-3p activates PI3K/AKT pathway. Western blot analysis was used to measure expressions of PI3K, phosphorylated AKT (p-AKT), AKT, p-ERK2, and ERK2 in neural cells. (A) The cells were transfected with control, bupivacaine, miR-489-3p mimic, or bupivacaine plus miR-489-3p. (B) The cells were transfected with control, bupivacaine, ASO-miR-489-3p mimic, or bupivacaine plus ASO-miR-489-3p. (C) and (D) show quantitative analysis of p-AKT and p-ERK expressions, respectively. PI3K: phosphoinositide 3-kinase; AKT: serine-threonine kinase; ERK: extracellular signal-regulated kinase-1; GAPDH: glyceraldehyde-3-phosphate dehydrogenase. * $P<0.05$, ** $P<0.01$.

neurons and promote apoptosis; addition of bupivacaine amplified these effects. In addition, we found that miR-489-3p and bupivacaine synergistically inhibited neurite growth. These results indicate that miR-489-3p plays an inhibitory role during the recovery process of SCI. Moreover, we confirmed that NAA10 is a target gene of miR-489-3p and is negatively regulated by miR-489-3p. Overexpression of NAA10 reversed the effects of miR-489-3p on neurons. Furthermore, we observed that the inhibitory effects of miR-489-3p on neurons are mediated via activation of the PI3K/AKT pathway. In all experiments, ASO-miR-489-3p (miR-489-3p inhibitor) could significantly reverse the effects of miR-489-3p and bupivacaine.

Overexpression of several miRNAs after SCI has been reported in previous studies also. In a murine transection model of SCI, miR-20a was notably increased in mouse SCI lesions as compared with normal spinal cord (Jee et al. 2012). Similar observation was noted for miR-486 in a murine contusion model of SCI: miR-486 was significantly overexpressed in injured spinal cord compared with normal spinal cord 7 days after SCI induction (Min et al. 2012). In another murine contusion model of SCI, miR-21 levels were highly increased around the lesion site after SCI (Bhalala et al. 2012). In the present study, we found that miR-489-3p is overexpressed in SCI patients as well as in bupivacaine-treated injured neurons.

The role of miR-489-3p in cell proliferation and apoptosis is known from previous literature. Patel et al. (2016), reported that miR-489 overexpression inhibited cell proliferation in breast cancer cell lines. Similar findings were reported by Zhang et al. (2016), who demonstrated that overexpression of miR-489 significantly suppressed cell proliferation and invasion in gastric cancer cells. In another study, miR-489 overexpression inhibited human ovarian cancer cell growth and induced apoptosis (Wu et al. 2014). In consistence with these results, we showed that miR-489-3p inhibits proliferation and promotes apoptosis of neural cells. In addition, we also found that miR-489-3p promotes apoptosis by increasing the expression of pro-apoptotic protein (Bax) and decreasing the expression of anti-apoptotic protein (Bcl-2).

MicroRNAs have an important role in regulation of neurite outgrowth during neuronal differentiation. Few miRNAs inhibit neurite outgrowth while others promote outgrowth. miR-127 has been reported to inhibit neurite outgrowth and induce apoptosis by regulating the expression of the mitochondrial membrane protein, mitoNEET (He et al. 2016). In contrast, Yu et al. (2008) reported that overexpression of miR-124 in differentiating mouse P19 cells promotes neurite outgrowth. In the present study, we found that overexpression of miR-489-3p inhibits neurite outgrowth by decreasing the expressions of GFAP and GPRIN1. GFAP is a major intermediate filament protein of mature astrocytes. Astrocytes are

a main type of glial cells in the CNS, and play a critical role in acute CNS trauma and neurodegenerative diseases (Hol and Pekny 2015). GRIN1 is expressed in the brain and interacts selectively with Gαo (activated α subunits of the Gi subfamily). It has been suggested that the Gαo-GRIN1 pathway could be involved in the regulation of neurite growth (Nakata and Kozasa 2005).

NAA10 is a gene important for normal cell function. MicroRNAs have been reported to target NAA10. Yang et al. (2015) showed that miRNA-342-5p and miR-608 inhibit colon cancer tumorigenesis by targeting NAA10. However, miR-489-3p has not been evaluated for this gene. The present study is the first to explore effects of miR-489-3p on NAA10. Using bioinformatic analysis, we predicted NAA10 as a target gene of miR-489-3p. Then, we examined the effect of miR-489-3p on NAA10 and found that NAA10 is downregulated by miR-489-3p in neurons. We also assessed whether NAA10 could affect neural cell proliferation, apoptosis and neurite outgrowth. The result suggested that NAA10 promotes cell proliferation and inhibits apoptosis in neural cells as well as promotes neurite outgrowth. Then, we assessed effect of NAA10 on GFAP and GPRIN1 expression and found that NAA10 promotes the expression of these synaptic growth marker proteins. These findings together indicate that miR-489-3p negatively regulate NAA10, which is responsible for neural cell proliferation and neurite outgrowth.

The PI3K/AKT signal pathway is an important pathway for various cellular processes, such as cell survival, proliferation, and migration (Chen et al. 2016). Recent studies have shown that the PI3K/AKT pathway is the main survival-promoting signal, and its activation is crucial in protecting nerve cells against ischemia and anoxia neuron damage (Guo et al. 2007; Oishi 2007; Qin et al. 2006; Renfu et al. 2014; Vicario-Abejón et al. 2000). Therefore, the expression of the PI3K/AKT pathway is increased after SCI. In a study in rats, the expression of PI3K, AKT and p-AKT showed a sharp increase one day after SCI, and then it decreased gradually, but the absolute expression was notably higher than that in the normal group (Zhang et al. 2014). In consistence with this finding, we demonstrated that the expressions of PI3K, p-AKT, and p-ERK2 are increased after neuron injury, induced by bupivacaine. We also showed that overexpression of miR-489-3p leads to increased expression of these proteins.

Furthermore, activation of the PI3K/AKT pathway in astrocytes is involved in the glial scar formation process. Glial scar may act as a physical and chemical barrier to axonal growth and limit neurite outgrowth. Thus, inhibition of the PI3K/AKT pathway may attenuate glial scar formation after SCI. In our study, we demonstrated that the miR-489-3p inhibitor could inhibit the expressions of PI3K, p-AKT, and p-ERK2 in neurons. This finding suggests that knockdown of miR-489-3p can be used as a therapeutic strategy for the treatment of SCI.

In conclusion, this study reveals that miR-489-3p is highly expressed after SCI, and is involved in inhibition of neural cell proliferation, induction of apoptosis, and inhibition of neurite outgrowth. We also identified NAA10 as target gene for miR-489-3p and demonstrated that NAA10 is negatively regulated by miR-489-3p. Finally, we showed that miR-489-3p activates the PI3K/AKT pathway which is involved in glial scar formation process and limit neurite outgrowth. The effects of miR-489-3p and bupivacaine were reversed by miR-489-3p inhibitor, suggesting a possible therapeutic strategy for SCI. Our research might provide a new insight into the prevention and treatment of SCI.

4. Experimental

4.1. Study subject and sample collection

A total of 20 patients with clinical and radiologic signs of cervical spondylotic myelopathy were selected between June 2011 and October 2012 from China-Japan Unior Hospital of Jilin University, and 20 healthy subjects were recruited as control. Disease duration ranged from 6 to 24 months. Exclusion criteria were: age >75 years; having heart, hepatic, renal or pulmonary diseases; and having peripheral vascular diseases affecting the upper limbs.

Blood samples for measurement of differential miR-489-3p expression between patients and controls were taken three days after surgery. Samples were inverted gently several times and were allowed to clot for 30 min at room temperature. Serum was obtained from blood samples centrifuged at 1500 rpm for 15 min and then stored at -80 °C before analysis. Then, expression level of miR-489-3p was measured in patient and control samples.

4.2. Cell culture and bupivacaine-induced neuronal injury

Human neural cell lines, AGE1.HN and SY-SH-5Y, were obtained from American Type Culture Collection (ATCC) and maintained at 37 °C in a humidified atmosphere of 5% CO_2 with MEM medium (Life Technologies), containing 10% fetal calf serum (Sigma-Aldrich, St Louis, MO, USA), 2 mM l-glutamine (Gibco BRL Co. Ltd., USA), and 100 U/mL penicillin/streptomycin (Gibco BRL Co. Ltd., USA).

To cause local anesthetic-induced neuronal injury in cultured neurons, various concentrations of bupivacaine (0, 0.5, 1, 2, 5, and 10 mM) were added into culture for 2 h, followed by 3×10 min washing with fresh culture medium. The neurons were then cultured for additional 24 h before further evaluation

4.3. Transfections of miR-489-3p mimic, ASO-miR-489-3p or NAA10-plasmid

The neural cells were grown to 80%-90% confluency and subsequent cultured in 6-well plate with 1×10^5 cells/well. After incubation for 3 h, cells were transfected with miR-489-3p mimic (10 mM), ASO-miR-489-3p (100 mM) or negative control, using Lipofectamine® 2000 (Invitrogen). For overexpression of N(alpha)-acetyltransferase 10 (NAA10) in the neural cells, cells were transfected with plasmid vector containing NAA10 gene (NAA10-plasmid) using Lipofectamine 2000 (Invitrogen) with blank plasmid as control.

4.4. Proliferation assay

Cell proliferation was determined using a 3-(4,5-dimethylthiazol-2-yl)-2 5-diphenyl-2H-tetrazolium bromide (MTT) assay. Briefly, cells were seeded in 96-well plates at a density of 2500 cells/well. At 24 h post transfection, 20 µL MTT reagent (5 mg/mL, Sigma-Aldrich, St Louis, MO, USA) was added to the test well and incubated at 37 °C for 4 h. Then the culture medium was removed and 150 µL dimethyl sulfoxide (DMSO, Sigma-Aldrich) was added to test well. The absorbance at 490 nm was measured using Thermo Scientific Multiskan (Thermo Fisher Scientific, USA).

4.5. Apoptosis assay

Cultured neurons were lifted and trypsinized into single cell suspension. After washing with ice-cold phosphatase buffer solution (PBS, Invitrogen, USA), the neurons were pooled and labeled with 10 mg/mL FITC-Annexin V (Becton Dickinson, USA) and 1 mg/mL propidium iodide. The mixture was incubated for 20 min and analyzed on a FACSCalibur cytometer (Becton Dickinson, USA).

4.6. Quantitative reverse transcription polymerase chain reaction (qRT-PCR)

Cultured neurons were lifted and trypsinized into single cell suspension. RNA was purified by a Trizol RNA purification Kit as per the manufacturer's protocol (Qiagen, USA). Total RNA concentrations were confirmed by a NanoDrop ND-3000 spectrophotometer (Fisher Scientific, USA) at 260 and 280 nm (A260/280) and analyzed by an Agilent 3100 Bioanalyzer (Agilent Technologies, USA). qRT-PCR was then conduced using a TaqMan miRNA assay as per the manufacturer's protocol (Applied Biosystems, USA), with primer sets to identify mature miR-489-3p. The amplification conditions were 30 cycles of 25 s at 91 °C and 3 min at 53 °C. The controls used in qRT-PCR were U6 for miRNA, and beta-actin for mRNA.

4.7. Western blot analysis

Cultured neurons were lifted and trypsinized into single cell suspension, then homogenized in a lysis buffer containing 50 mM Tris (pH 7.6), 150 mM NaCl, 1 mM EDTA, 10% glycerol, 0.5% NP-40 and protease inhibitor cocktail (Invitrogen, USA). The total protein were separated on a 10% sodium dodecyl sulfate polyacrylamide gel electrophoresis (SDS-PAGE) gradient gel (Bio-Rad, USA) and transferred to polyvinylidene difluoride (PVDF) filters (Invitrogen, USA). The blots were blocked with 5% dry-milk for 1 h, followed by incubation of primary antibodies overnight at 4 °C. Horseradish peroxidase-conjugated secondary antibody (Bio-Rad, USA) was applied for another 1 h at room temperature, and glyceraldehyde 3-phosphate dehydrogenase (GAPDH) was used as loading control. The blot was then developed by an enhanced chemiluminesence system (Amersham Biosciences, USA) as per the manufacturer's protocol.

4.8. Neurite outgrowth assay

To measure neurite outgrowth, three days after bupivacaine treatment, neurons were fixed with 4% paraformaldehyde in PBS for 1 h, followed by 3×10 min wash with PBS. Neurons were blocked with 4% donkey serum and 0.1% Triton in PBS for another hour, and then incubated with anti-neurofilament antibody (1:500, Santa Cruz Technology, USA) at 4°C overnight. On the second day, neurons were incubated with Alexa Fluor 488-conjugated secondary antibody (1:500, Invitrogen, USA) at room temperature for 1 h. The average length of the twenty longest neurites under each experimental condition was measured using ImageJ (NIH) software and normalized to the averaged length under control condition (0 mM bupivacaine).

4.9. Dual luciferase reporter assay

The neural cells were plated at (0.5-1)×10^4 per well in 24-well plates. On the next day, 100 ng pGL3-NAA10 plasmids were co-transfected with miR-489-3p mimic or ASO-miR-489-3p into cells using Lipofectamine 2000 (Invitrogen) for 3'-UTR reporter activity assay. After 48 h, cells were harvested and luciferase assays were performed using Dual Luciferase Reporter Assay system (Promega Corp., WI, USA).

4.10. Statistical analysis

All data are expressed as mean±standard deviation (means±SD) from triplicate experiments and were analyzed with SPSS software (version 16.0; SPSS Inc., Chicago, Illinois, United States). All variables were compared with Student's t-test or one-way analysis of variance (ANOVA), followed by Newman-Keuls post-hoc analysis. A p value less than 0.05 was considered to be statistically significant.

Acknowledgement: The work was not supported by any funding agency.

Conflict of interest: The authors declared no conflict of interests.

References

Bareyre FM (2008) Neuronal repair and replacement in spinal cord injury. J Neurol Sci 265: 63–72.

Bartel DP (2004) MicroRNAs: genomics, biogenesis, mechanism, and function. Cell 116: 281–297.

Bhalala OG, Pan L, Sahni V, Mcguire TL, Gruner K, Tourtellotte WG, Kessler JA (2012) microRNA-21 regulates astrocytic response following spinal cord injury. J Neurosci 32: 17935-17947.

Bhalala OG, Srikanth M, Kessler JA (2013) The emerging roles of microRNAs in CNS injuries. Nature Rev Neurol 9: 328-339.

Calvo M, Zhu N, Grist J, Ma Z, Loeb JA, Bennett DLH (2011) Following nerve injury neuregulin-1 drives microglial proliferation and neuropathic pain via the MEK/ERK pathway. Glia 59: 554-568.

Chen CH, Sung CS, Huang SY, Feng CW, Hung HC, Yang SN, Chen NF, Tai MH, Wen ZH, Chen WF (2016) The role of the PI3K/Akt/mTOR pathway in glial scar formation following spinal cord injury. Exp Neurol 278: 27-41.

Donnelly DJ, Popovich PG (2008) Inflammation and its role in neuroprotection, axonal regeneration and functional recovery after spinal cord injury. Exp Neurol 209: 378-388.

Guo JS, Zeng YS, Li HB, Huang WL, Liu RY, Li XB, Ding Y, Wu LZ, Cai DZ (2007) Cotransplant of neural stem cells and NT-3 gene modified Schwann cells promote the recovery of transected spinal cord injury. Spinal Cord 45: 15-24.

He QQ, Xiong LL, Liu F, He X, Feng GY, Shang FF, Xia QJ, Wang YC, Qiu DL, Luo CZ (2016) MicroRNA-127 targeting of mitoNEET inhibits neurite outgrowth, induces cell apoptosis and contributes to physiological dysfunction after spinal cord transection. Sci Reports 6.

Hol EM, Pekny M (2015) Glial fibrillary acidic protein (GFAP) and the astrocyte intermediate filament system in diseases of the central nervous system. Curr Opin Cell Biol 32: 121-130.

Hutchison ER, Okun E, Mattson MP (2009) The therapeutic potential of microRNAs in nervous system damage, degeneration and repair. NeuroMolecular Medicine 11: 153-161.

Jee MK, Jung JS, Im YB, Jung SJ, Kang SK (2012) Silencing of miR20a is crucial for Ngn1-mediated neuroprotection in injured spinal cord. Human Gene Ther 23: 508-520.

Liu Q, Yang G, Qian Y (2016) Loss of MicroRNA-489-3p promotes osteosarcoma metastasis by activating PAX3-MET pathway. Mol Carcinog doi: 10.1002/mc.22593.

Min KJ, Jin SJ, Inchoi J, Jin AJ, Sunkang K, Binim Y, Kyungkang S (2012) MicroRNA 486 is a potentially novel target for the treatment of spinal cord injury. Brain 135: 1237-1252.

Nai-Kui Liu X-FW, Qing-Bo Lu, Xiao-Ming Xu (2009) Altered MicroRNA Expression following Traumatic Spinal Cord Injury. Exp Neurol 219: 424-429.

Nakata H, Kozasa T (2005) Functional Characterization of Gαo Signaling through G Protein-Regulated Inducer of Neurite Outgrowth 1. Mol Pharmacol 67: 695-702.

Oishi Y (2007) BDNF, NT-3, and NGF released from transplanted neural progenitor cells promote corticospinal axon growth in organotypic cocultures. Spine 32: 1272-1278.

Patel Y, Shah N, Ji SL, Markoutsa E, Jie C, Shou L, Botbyl R, Reisman D, Xu P, Chen H (2016) A novel double-negative feedback loop between miR-489 and the HER2-SHP2-MAPK signaling axis regulates breast cancer cell proliferation and tumor growth. Oncotarget 7: 18295-18308.

Qin DX, Zou XL, Luo W, Zhang W, Zhang HT, Li XL, Zhang H, Wang XY, Wang TH (2006) Expression of some neurotrophins in the spinal motoneurons after cord hemisection in adult rats. Neurosci Lett 410: 222-227.

Renfu Q, Rongliang C, Mengxuan D, Liang Z, Jinwei X, Zongbao Y, Disheng Y (2014) Anti-apoptotic signal transduction mechanism of electroacupuncture in acute spinal cord injury. Acupunct Med 32: 463-471.

Slezak-Prochazka I, Durmus S, Kroesen BJ, Van dBA (2010) MicroRNAs, macrocontrol: regulation of miRNA processing. RNA 16: 1087-1095.

Vicario-Abejón C, Collin C, Tsoulfas P, Mckay RDG (2000) Hippocampal stem cells differentiate into excitatory and inhibitory neurons. Eur J Neurosci 12: 677-688.

Wang K, Liu F, Zhou LY, Long B, Yuan SM, Wang Y, Liu CY, Sun T, Zhang XJ, Li PF (2014) The long noncoding RNA CHRF regulates cardiac hypertrophy by targeting miR-489. Circ Res 114: 1377-1388.

Wu D, Murashov AK (2013) Molecular mechanisms of peripheral nerve regeneration: emerging roles of microRNAs. Frontiers Physiol 4: 55.

Wu H, Xiao Z, Zhang H, Wang K, Liu W, Hao Q (2014) MiR-489 modulates cisplatin resistance in human ovarian cancer cells by targeting Akt3. Anti-Cancer Drugs 25: 799-809.

Xie Z, Cai L, Li R, Zheng J, Wu H, Yang X, Li H, Wang Z (2015) Down-regulation of miR-489 contributes into NSCLC cell invasion through targeting SUZ12. Tumor Biol 36: 6497-6505.

Yang H, Li Q, Niu J, Li B, Jiang D, Wan Z, Yang Q, Jiang F, Wei P, Bai S (2015) microRNA-342-5p and miR-608 inhibit colon cancer tumorigenesis by targeting NAA10. Oncotarget 7: 2709-2720.

Yu JY, Chung KH, Deo M, Thompson RC, Turner DL (2008) MicroRNA miR-124 regulates neurite outgrowth during neuronal differentiation. Exp Cell Res 314: 2618-2633.

Zhang B, Ji S, Ma F, Ma Q, Lu X, Chen X (2016) miR-489 acts as a tumor suppressor in human gastric cancer by targeting PROX1. Am J Cancer Res 6: 2021-2030.

Zhang P, Zhang L, Zhu L, Chen F, Zhou S, Tian T, Zhang Y, Jiang X, Li X, Zhang C (2014) The change tendency of PI3K/Akt pathway after spinal cord injury. Am J Transl Res 7: 2223-2232.